# Adjustments of Analytical Simplified Methods to Estimate the Effective Thermal Resistance of Masonry Walls

Maysoun Ismaiel[1], Yuxiang Chen[1]
[1] University of Alberta, Edmonton, Canada

## Abstract

Determining the effective thermal resistance of masonry veneer walls is not a simple technique due to the thermal bridging effect. The lateral heat flows caused by highly conductive elements penetrating the insulation layer (e.g., ties) allow heat to be transferred in multiple directions that are considered a challenge in the R-value estimations. Energy savings and improved structural durability can be achieved through applying design considerations that address the thermal bridging effect. Therefore, this paper aims to suggest an adjustment of current thermal resistance estimation methods (i.e., isothermal planes and parallel path methods) to include the thermal bridging effects resulting from veneer ties in the effective R-value estimations. The analytical R-values obtained using the adjustments were compared with numerical simulations using a 3D steady-state finite element method (FEM) in addition to experimental validation obtained from the literature.

## Introduction

In the transition to sustainable buildings, modern concrete blocks and masonry veneers can be a significant constituent. Masonry is aesthetically pleasing and is energy efficient and durable (Ismaiel et al., 2021). In Canada, a significant change in the calculation method for overall thermal transmittance was presented by the National Energy Code of Buildings (NECB, 2017). The exclusion of major structural elements and other elements that penetrate the envelope as long as they made up less than 2% of the wall area is no longer accepted. The new calculation method requires considering all thermal bridging elements into the effective R-value calculations along with the major structural elements such as balconies, beams and columns. This change requires the use of new methods and tools to calculate envelope thermal resistance values accurately and account for all thermal bridges in the envelope. To comply with these continuously evolving challenges and energy code requirements, the masonry construction industries are looking for an effective approach for thermal resistance calculation to help in the improvement of the thermal design of masonry walls, and hence reduce the energy consumption of buildings. The configurations of the masonry wall assemblies play a key role in the walls' thermal performance. One of the challenges in the assembly configuration is the thermal bridging which takes place where highly conductive structural components penetrate insulating materials, such as at the structural members' penetrations through the insulation plane (e.g., veneer ties) (CCMPA, 2013). Traditional steel masonry veneer ties are among the sources of thermal bridging in concrete masonry walls (Adam Di Placido et al., 2019). This paper focuses on estimating the impact of heat flow through clear walls without intersections of the primary structure or between assemblies. The typical components of concrete masonry clear walls are concrete blocks, mortar, insulation boards, veneer ties, and air gap in the case of brick veneer masonry walls. Figure 1 shows the main clear wall components addressed in this study.

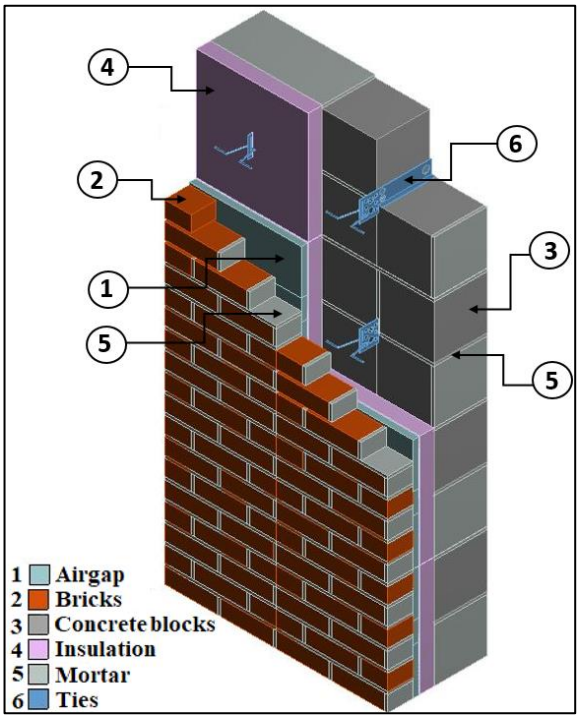


*Figure 1: Components of clear masonry veneer walls*

This paper aims to suggest adjustments of current thermal resistance estimation methods (i.e., isothermal plane and parallel path methods) to be applied on exterior masonry veneer walls considering the effect of the thermal bridging caused by the veneer ties. The significance of such work would help designers to estimate quickly and accurately the thermal bridging effect caused by the veneer ties. In addition, accurate estimations of R-values will help with reliable estimation of energy needs for the buildings, improvements to the thermal envelope and in the calculation

of required heating ventilation and air conditioning (HVAC) equipment.

This paper is structured as follows, after the introduction section; a brief discussion of the commonly used thermal resistance estimation methods is presented. This is followed by a description of the finite element models used in this study. Then, a presentation of the suggested method and application of the suggested adjustments along with a comparison with the finite element simulation results is presented. Finally, the results and main concluding remarks are discussed.

**Analytical Simplified Methods**

Series and parallel path methods are two of the most commonly used techniques for thermal resistance calculations. In the case of the series path method, the heat flows layer by layer through a building assembly made of multiple materials stacked together. Accordingly, in series flow paths, the thermal resistance of a building assembly composed of uniform parallel layers consists of the sum of the resistances of all layers in series (ASHRAE, 2017a). In the case of the parallel path method, the heat flows through different pathways and is assumed to be transferred in parallel paths of different conductance. If no heat flows through lateral paths in a building assembly, the parallel path method is applied by assuming one-dimensional heat transfer perpendicular to the surfaces of the building element. This assumption is accurate when the materials on the same layer are having close thermal conductivity values (i.e., wood frame walls). Most building assemblies are a combination of layers in series and parallel. Therefore, a combination of both methods is also used called the series-parallel (e.g. isothermal planes) method. In the isothermal planes method, it is assumed that the heat can flow laterally in any component and the thermal resistances of adjacent components are combined in parallel, resulting in a path with series-parallel resistance combined (ASHRAE, 2017b). The parallel and isothermal-planes methods are often considered two separate calculation methods. Recently, The ASHRAE Handbook Fundamentals (ASHRAE, 2017b) suggested the actual R-value lies between both methods. The ASHRAE Fundamentals Handbook (ASHRAE, 1993a) suggested that these methods provide a range of upper and lower limits on the true thermal resistance. However, The ASHRAE Fundamentals Handbook (ASHRAE, 1993a) generally recommended further experimental examinations of the required studied elements to reveal whether the actual thermal resistance value closer to the higher or lower calculated range. Another method is described in the International Standards ISO 6946 (ISO, 1995). This method is used to compute the thermal resistance of building elements consisting of homogeneous and inhomogeneous layers. The combined method suggests computing the total thermal resistance as an arithmetic average of the upper and lower thermal resistances limits obtained using the parallel path and the isothermal planes methods respectively. However, there are some limitations to this method; (1) this approach is only applicable in the case of the ratio of the upper limit to the lower limit of the thermal resistance does not exceed 1.5. (2) this method is not valid in cases of thermal insulation is bridged by metal and in the cases where there is a significant difference between the thermal conductivity of the materials in the same layer. (3) there are some corrections required to the thermal transmittance values for air voids, mechanical fasteners, and inverted roofs. These previous studies and methods aimed to have an accurate estimation of the overall R-value for different assemblies and cases. However, the literature showed that further methods are required to consider the overall R-value in the assemblies where thermal insulation is bridged by metal with a significant difference between the thermal conductivity of the materials in the same layer.

## Methodology

This study investigates the thermal resistance of clear masonry wall assemblies analytically based on 3D finite element computer modelling (ANSYS). The objective of this study is to suggest an adjustment of current thermal resistance estimation methods (isothermal plane and parallel path methods) to include the effect of the thermal bridge resulting from veneer ties on the total masonry walls' R-value estimations. This section presents the Finite Element simulations used in this study. Then, a detailed description of the models and the suggested adjustments is presented.

**Finite Element Analysis Simulations**

ANSYS Workbench (ANSYS, 2019) was used to perform steady-state finite element thermal analysis simulations of typical brick veneer cavity wall assemblies. There are some modelling assumptions considered in this study; all models were analyzed at a steady-state thermal analysis and air leakage was not considered. The models were evaluated at -18C$^{o}$ is the exterior temperature and 21 C$^{o}$ is the interior. Contact resistance was not considered in the stimulations because all models addressed are clear wall models. Therefore, contact resistance has a minimum effect on the walls' thermal resistance (Roppel et al., 2011). All the material properties were considered from the ASHRAE Handbook (ASHRAE, 2019). The element used to simulate the wall components in the ANSYS modelling is SOLID70 based on its properties which complies well with the assemblies required to be investigated. SOLID70 has a three-dimensional thermal conduction capability. The element has eight nodes with a single degree of freedom, and temperature, at each node. The element can be applied to a three-dimensional, steady-state or transient thermal analysis. Meshing was done by using ANSYS's advanced sizing feature. A mesh was generated that is relatively fine for specific parts of the model (such as the ties). A sequence of mesh convergence tests had been conducted for a suitable balance between accuracy and computational time of the

addressed models. The convergence study on the mesh size was carried out by evaluating the variation of the heat flux versus the number of mesh nodes. It was found that the mesh size of 10 mm is appropriate for the accuracy and model running time for all studied cases.

From the results of the numerical modelling, an R-value was obtained for the overall wall. This R-value was determined from the overall heat transfer through the wall for defined internal and external environmental temperatures as mentioned earlier, as follows:

$$R = \frac{\Delta T}{q} \quad (1)$$

where: $q$ is the heat flux in watts per area of the addressed wall in square meters ($W/m^2$) as predicted by the modelling, and $\Delta T$ is the difference in temperature between the inside and outside environment.

**Models and Adjustments Description**

First, simplified finite element models (Type A) were addressed. Type A models represent the current common brick veneer tie types used in practice; block ties (shown in Figure 2). 60,000 simplified models (Type A) were simulated (shown in Figure 3). ANSYS workbench was used to perform steady-state thermal finite element simulations to address variables such as the thermal conductivity and the dimensions of each component of the wall.

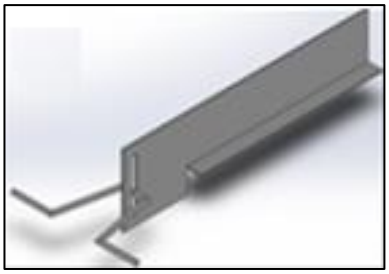

*Figure 2: Masonry block veneer tie*

The simplified configurations (Type A) were considered a preliminary phase to address the suggested R-value adjustments. Type A models were used to simplify the clear wall geometry into regular shapes connected in series and parallel connections. In addition, the effect of one tie only was considered in the center of each assembly. Layers A, B, C, D and F represent concrete blocks, insulation boards, tie, air gap and brick veneer, respectively. $L_A$, $L_B$, $L_C$, $L_D$ and $L_F$ represent the thickness (m) of concrete blocks, Insulation boards, tie, air gap and brick veneer, respectively. Table 1 shows the range of dimensions used for each layer as well as the thermal conductivity range considered for each addressed layer.

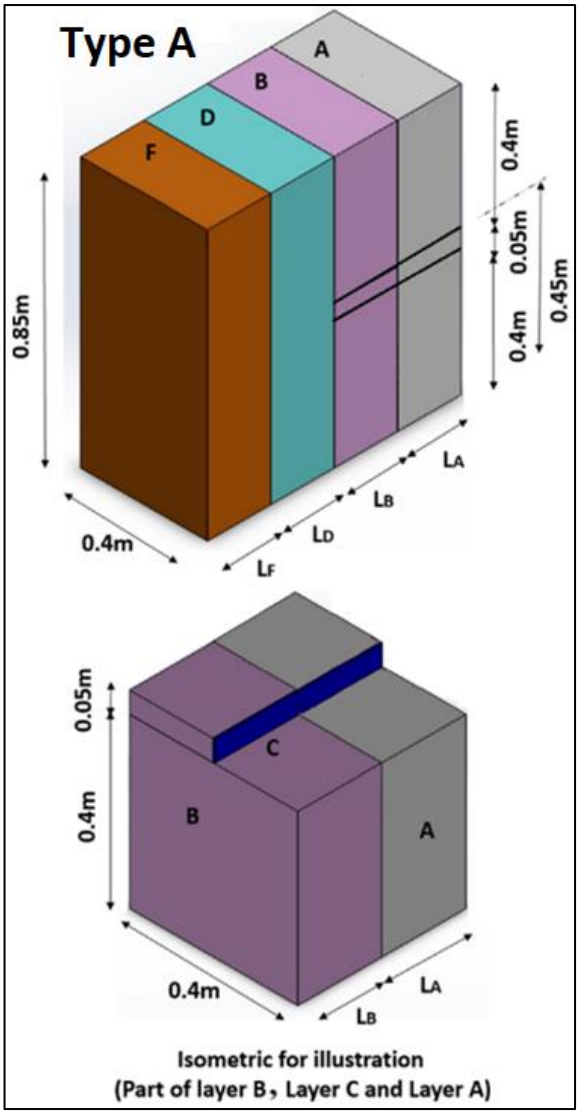


*Figure 3: Simplified assemblies, Type A representing block tie type*

*Table 1: The range of dimensions and thermal conductivity used for each layer*

| Layer | Represents | Thermal Conductivity range (W/m K) | Thickness range (m) |
|---|---|---|---|
| A | Concrete blocks* | 0.185 - 0.445 | 0.09 - 0.3 |
| B | Insulation boards | 0.02 - 0.07 | 0.025 - 0.15 |
| C | Ties | 50 - 0.2 | 0.002 - 0.01 |
| D | Air gap | 0.0415 - 0.7 | 0.025 - 0.15 |
| F | Brick veneer | 0.405 - 1.34 | 0.07 - 0.3 |

*The considered range of the thermal conductivity of the concrete blocks reflects the cases of un-grouted (Hollow) and fully grouted concrete blocks in the simplified models' simulations

Isothermal and parallel thermal circuits were developed for Type A configurations as shown in Figure 4. In addition to addressing serval variables as mentioned in Table 1, the significance of addressing simplified models in the preliminary stage also includes saving the immense execution and simulation time that detailed assemblies require. Using traditional calculation methods along with the finite element simulations results facilitates comparing the results obtained from the suggested adjustments.

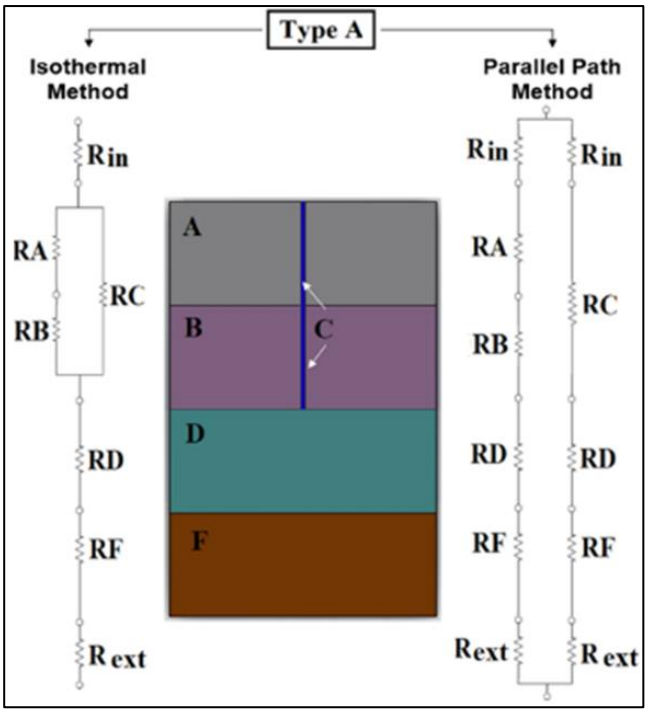


*Figure 4: Equivalent isothermal and parallel thermal circuit for Type A assemblies (Note: $R_{in}$ and $R_{ext}$ are the interior and exterior air film resistance)*

Then, detailed clear masonry wall models were constructed (Type B) as shown in Figure 5 . 180 detailed clear masonry wall finite element models were simulated using ANSYS. The detailed finite element models represent two types of the currently used brick veneer ties in practice; solid block ties (Type $B_1$) and slotted block ties (Type $B_2$).

Table 2 presents the fixed material properties for all the studied schemes. An interior and exterior air film were considered in analysis for all models with the nominal resistance of 0.11 and 0.03 $m^2K/W$ respectively. The thermal resistance of the air gap, 0.07 $m^2K/W$, between the wall thermal insulation and the brick veneer was obtained from the ASHRAE Handbook and literature (ASHRAE, 2019; Hershfield, 2016). 180 models (2 types of ties x 3 tie materials x 3 insulation R-value x 2 grout conditions x 5 block densities = 180) were studied for type B to discuss different variables. Table 3 presents the variables considered for each studied scheme.

*Table 2: Material thickness and properties used in the studied schemes for Type B models*

| Component | Thickness (mm) | Conductivity (W/m K) |
|---|---|---|
| Standard concrete Block Size Block 390X190X190 mm (Size block no.20) (Sturgeon et al., 2013a; Sturgeon et al., 2013b) | 190 | Varies |
| Cement Mortar | 10 | 1.2 |
| Masonry ties (400mm on centre) * | 14 gauge | Varies |
| Insulation | 50 | Varies |
| Brick veneer | 90 | 0.81 |

*There are several spacings of the masonry ties used in the market based on the structural requirements of the addressed wall. This study focuses on the minimum masonry tie spacing to address the worst case of the masonry tie thermal bridging effect.

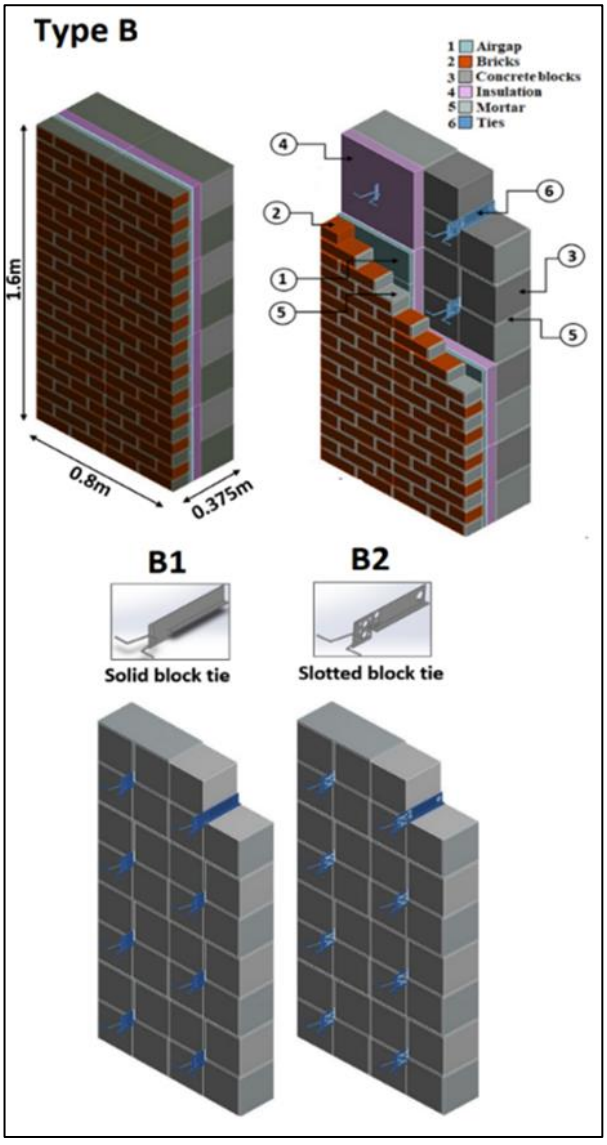

*Figure 5: Detailed assemblies, Type $B_1$ and $B_2$ - Note: Since the walls' geometry is symmetrical, the geometrical complexity of the model was reduced by simulating only one tie and simplifying the total dimensions of the simulated model to be (400 X 400 X 375mm)*

*Table 3: The variables considered in each studied scheme*

| Scheme | Variables considered |
|---|---|
| General variables considered for each assembly | Tie type, tie material, insulation R-value, concrete block density, concrete block type |
| R-values in BTU/(ft2·°F·hr) and in (m2K/W) for insulation | R-15 (2.64), R-20 (3.52), R-25 (4.40) |
| Block Density (kg/m3) (conductivity (k=W/m K) | Hollowed: 2100(k=1.17), 1800(k=0.87), 1550(k=0.66), 1380 (k=0.6), 1150(k=0.35) Fully grouted: 2100(k=1.9), 1800(k=1.13), 1550(k=0.78), 1380(k=0.6), 1150(k=0.36) |
| Type of wall | Hollow block wall, Fully grouted wall |
| Tie type | Block solid tie, Block slotted tie |
| Ties materials (conductivity =W/m K) | Galvanized steel (k=50), Stainless steel (k=17), GFRP (k=0.2) |

Equivalent isothermal and parallel thermal circuits were developed for Type B assemblies as shown in Figure 6. Alternate shorted paths were considered by combing similar elements in each layer to reduce the number of paths. The V-Tie (the wire which anchors into the brick) was modelled and results showed that the V-tie didn't contribute significantly to thermal bridging. Therefore, the V-tie was ignored in the equivalent thermal circuits to simplify the calculations. In the case of addressing slotted (perforated) tie type (assemblies' type $B_2$); the tie area perpendicular to the thermal flow was multiplied by factor $F_{slotted}$ presented in equation (2) to consider the thermal transfer reduction effect caused by the slots.

$$F_{Slotted}=\frac{Volume\ of\ the\ slotted\ tie}{Volume\ of\ the\ sloid\ tie} \quad (2)$$

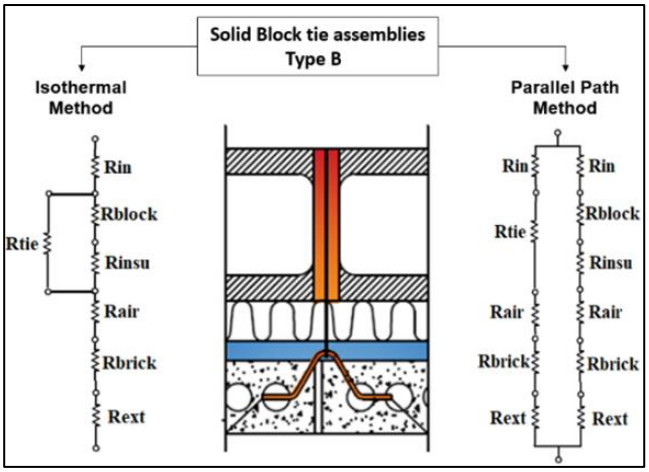


*Figure 6: Equivalent isothermal and parallel thermal circuits for Type B assemblies (Note: $R_{in}$ and $R_{ext}$ are the interior and exterior air film resistance)*

## Results

After the simplified assemblies, (Type A) R-value was estimated by using the parallel path, isothermal and FEM simulations. Results showed that the finite element results are between the results obtained from the isothermal analysis and the parallel path method. This observation complies well with The ASHRAE Fundamentals Handbook (ASHRAE, 1993a) suggestion, that these methods provide a range of upper and lower limits on the true thermal resistance. In addition, a comparison between R-values obtained from the parallel-path and isothermal-planes methods with respect to the R-values obtained by using finite element analysis was performed. A correlation matrix was constructed to address the strength of the relationship between significant variables (i.e., thermal conductivity, area of ties and insulation) and the difference between R-values results obtained from the parallel-path versus FE results and isothermal methods versus FE results. The correlation results showed that the ties and insulation thermal conductivities have the strongest correlation with the difference between the R-values addressed. Therefore, based on the ratio between the summation of thermal conductivities of layers penetrated by the thermal bridging source and the thermal conductivity of the thermal bridging source shown in equation (3), the actual R-values could be predicted whether closer to the isothermal plane method or the parallel path method.

$$Ratio=\frac{\sum K_i}{K_{TBS}} \quad (3)$$

Where; $K_i$ is the summation of thermal conductivities of layers penetrated by the thermal bridging source (W/m k) and $K_{TBS}$ is the thermal conductivity of the thermal bridging source (W/m k)

The FE results showed that for assemblies with a Ratio $\leq$ 0.1, the actual R-values results are closer to the parallel path method. While in the cases of Ratio $>$ 0.1, There was no significant difference recorded between the isothermal method and the parallel path method, both methods obtain the same results. Therefore, it was concluded that the combined method suggestions described in the International Standards ISO 6946 (ISO, 1995)-which states that "the total thermal resistance is computed as an arithmetic average of the thermal resistances obtained using the parallel path and the isothermal planes methods"- is valid for masonry veneer walls with Ratio > 0.1. Figure 7 shows the relation between the average R-value results obtained from the isothermal, parallel path and FE method (ANSYS) to the "Ratio" calculated from equation (3).

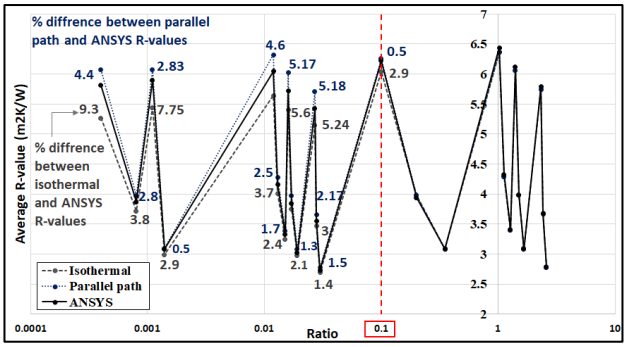


*Figure 7: R-value results using isothermal, parallel path and ANSYS with respect to the Ratio*

Using FEM results, adjustment factors were deduced by a procedure that is executed iteratively by comparing various solutions until a satisfactory solution is achieved. The optimization technique used in this study was based on setting the design objective to minimize the resulting difference between the values obtained by using the suggested adjustments and the actual values obtained by the FEM simulations. The accuracy of the presented R-value multipliers was investigated by computing the coefficient of determination $R^2$ for the Type A assemblies which is equal to 0.96 and the average error percentage between the FE results and the suggested results was 4%. While the average difference percentage between the results obtained by the parallel path and isothermal methods compared to the FEM results was 7% ($R^2$=0.94) and 12% ($R^2$=0.87), respectively. Factors of α and β shown in Table 4 were suggested based on the ratio shown in equation (2) the suggested R-value equation is as follows:

$$R_{adjusted} = \frac{\alpha * R_{isothermal} + \beta * R_{parallel}}{2} \qquad (4)$$

where; α and β are the adjustment factors for the R-value obtained using the isothermal method and the parallel path method respectively.

*Table 4: Adjustment factors*

| | **Ratio ≤ 0.01** | **0.01 < Ratio ≤ 0.1** | **Ratio > 0.1** |
|---|---|---|---|
| α | 1.12 | 1.21 | 1 |
| β | 0.91 | 0.77 | 1 |

The detailed configurations Type B were analyzed by using FEM simulations (ANSYS) and the suggested adjustment factors shown above in Table 4. The R-values' results obtained from both methods were compared. The average difference percentage between the results obtained by the adjustments and the FEM results is 2.14 % ($R^2$= 0.98). While the average difference percentage between the results obtained by the parallel path and isothermal methods compared to the FEM results were 25.5% ($R^2$= 0.7) and 19% ($R^2$= 0.8), respectively. Figure 8 shows the thermal distribution and the heat flux for one-studied case of models Type A. Figure 9 shows a comparison of the suggested adjustments with respect to the finite element simulation results. Figure 10 shows the thermal distribution and the heat flux for one-studied case of models Type B.

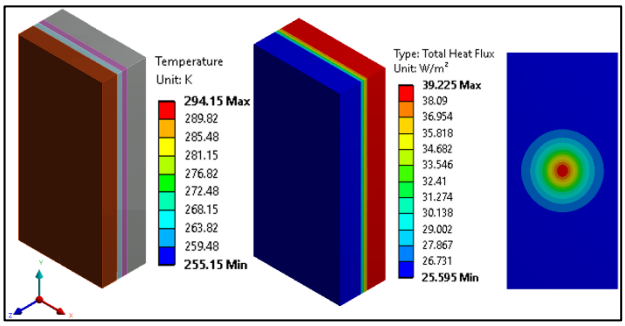


*Figure 8: Thermal distribution and the heat flux for one-studied case of models type A*

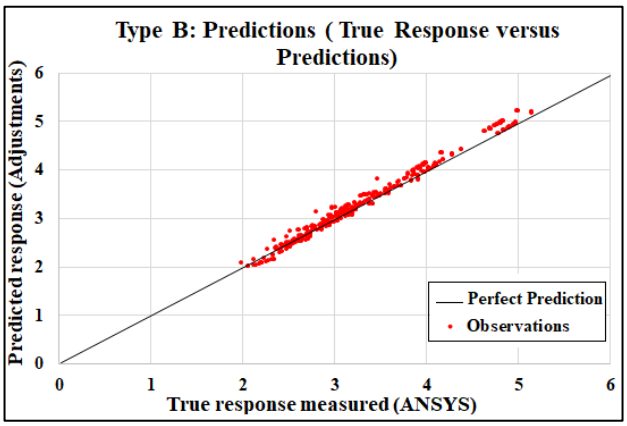


*Figure 9: Adjusted method with respect to the finite element modelling results for assemblies' type B*

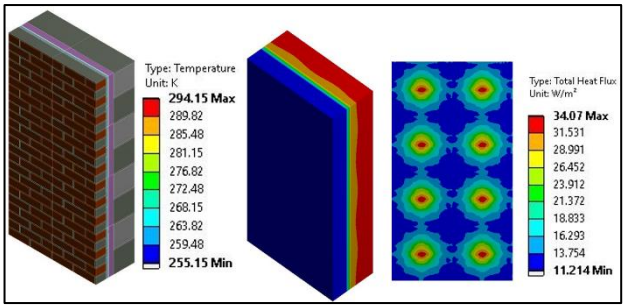


*Figure 10: Thermal distribution and the heat flux for one-studied case of models type B*

## Conclusion

The ratio between the summation of thermal conductivities of layers penetrated by the thermal bridging source and the thermal conductivity of the thermal bridging source is a useful basis for estimating R-values for masonry walls with veneer ties. Guiding ratios were presented for predicting whether the actual R-values are closer to the parallel path results or the isothermal results in the case of the presence of a thermal bridging source based on the conductivity of the thermal bridging sources and the penetrated layers. Results showed that in the case of having a low conductive element penetrating the insulation layer, the results will be

the same regardless of using the parallel path method or the isothermal plan method. Also, it was concluded that the finite element simulation results were closer to the average of the isothermal and the parallel path methods in case of the ratio between the summation of thermal conductivities of layers penetrated by the thermal bridging source and the thermal conductivity of the thermal bridging source is more than 0.1. The R-values' results obtained from the current thermal resistance estimation methods (i.e., isothermal planes and parallel path methods) were compared. The average difference percentage of the results obtained by the adjustments and the FEM is 2.14%. While the average difference percentage between the results obtained by the parallel path and isothermal methods compared to the FEM results was 25.5% and 19%, respectively. The suggested adjustment factors show good agreement with modelled results.

## Acknowledgement

This work was supported by the Natural Sciences and Engineering Research Council of Canada (NSERC), the Canadian Concrete Masonry Producers Association (CCMPA), and the Masonry Contractors Association of Alberta (MCAA).

## References

Adam Di Placido P, Chong D and Schumacher C (2019) Thermal evaluation of masonry shelf angle supports for exterior-insulated walls. *ASHRAE Topical Conference Proceedings.* American Society of Heating, Refrigeration and Air Conditioning Engineers, Inc., 309-317.

ANSYS (2019) *https://www.ansys.com/products/platform*.

ASHRAE (1993a) ASHRAE Handbook-Fundamentals, chapter 22. Atlanta. Ga.: American Society of Heating, Refrigerating and Air-Conditioning Engineers, Inc.

ASHRAE (2017a) 25.2.1.3 Heat Flow across an Air Space. *2017 ASHRAE® Handbook - Fundamentals (SI Edition)*. American Society of Heating, Refrigerating and Air-Conditioning Engineers, Inc. (ASHRAE), pp.6.

ASHRAE (2017b) 25.2.1.7 Series and Parallel Heat Flow Paths. *2017 ASHRAE® Handbook - Fundamentals (SI Edition)*. American Society of Heating, Refrigerating and Air-Conditioning Engineers, Inc. (ASHRAE), pp.7.

ASHRAE (2019) ASHRAE 90.1- Energy Standard for Buildings except Low-Rise Residential Buildings. Vol. Vol. 90 ASHRAE.

CCMPA (2013) Canadian Concrete Masonry Producers' Association-Thermal Properties & Design Details. *Technical Notes- Retrieved from:* https://ccmpa.ca/download/metric-technical-manual/6-thermprop/.

Hershfield M (2016) Building Envelope Thermal Bridging Guide, version 1.1. Hydro Power Smart. Vancouver, Canada.

Ismaiel M, Chen Y, Cruz-Noguez C, et al. (2021) Thermal resistance of masonry walls: a literature review on influence factors, evaluation, and improvement. *Journal of Building Physics*. 17442591211009549.

ISO (1995) International Standard ISO/DIS 6946-1, Thermal resistance and thermal transmittance of building components and building elements. Geneva: International Organization for Standardization.

NECB (2017) The national energy code of canada for buildings.

Roppel P, Hershfield M, Marif W, et al. (2011) Research Project Report RP-1365: Thermal Performance of Buildings Envelope Details for Mid and High-Rise Buildings. *ASHRAE Inc.* Report No. 5085243.01.

Sturgeon G, Eng B and Eng P (2013a) Coursing Tables, Metric Shapes and Sizes.

Sturgeon G, Eng B and Eng P (2013b) Physical Properties. Retrieved from Canadian Concrete Masonry Producers Association: Metric ….